Jurnal Kejuruteraan 36(2) 2024: 447–453
https://doi.org/10.17576/jkukm-2024-36(2)-06

Winding Response under Difference Effective Inductance for Single Phase High Voltage Transformer

Ramizi Mohamed[a*], Syahirah Abd Halim[a] & Paul L. Lewin[b]

[a]*Department of Electrical, Electronic and Systems Engineering, Faculty of Engineering & Built Environment, Universiti Kebangsaan Malaysia, Malaysia*

[b]*School of Electronics and Computer Science, University of Southampton, Southampton, SO17 1BJ, United Kingdom*

[*]*Corresponding author: ramizi@ukm.edu.my*

Received 15 March 2023, Received in revised form 3 August 2023
Accepted 3 September 2023, Available online 30 March 2024

ABSTRACT

Early studies of transformer winding parameters were focused on the determination via its physical dimensions and empirical formulas. In most cases it is divided into several parts namely coil section pairs, coils distance, disc coils diameter and thickness of insulation. Maxwell's equations are often the solution to the problem, which satisfy related boundary conditions between conductors for mutual inductance and capacitor equations. Such solutions often led to errors and hence its mathematical model. To counter the problem, it was suggested that such approximations must be conducted with experimental model windings at the same time. Frequency domain measurements and time domain measurements can be conducted to effectively determine these parameters. This in turn will investigate the behaviour of transformer winding electromagnetic transient at high frequency. From theoretical point of view, predominantly capacitive winding model often considered to represent its behaviour at high frequency and will give the results of its initial distribution. Under this consideration, a single phase plain winding is considered for investigation. A single rectangular wave was considered to represent infinitive impinge incident wave, injected at one end of transformer winding and the measured response signals of the wavetail were considered for measurement. The experimental response and modelling results were compared and proved to have high agreement between the two.

Keywords: Winding transformer; Capacitive winding; Transformer winding distribution.

INTRODUCTION

A large power transformer may consist of several main elements namely large transformer coil and transformer core. Fundamentally, a transformer consists of high voltage windings and low voltage windings, wrapped with selected insulation materials and surrounds laminated core. The windings can be represented with equivalent electrical parameter component called lumped parameter circuit model (Al-Kraimeen, 2019; Cheng et al. 2020; Ding et al. 2020; Mohamed & Lewin, 2011; Nia et al. 2020). Among those parameters under consideration are resistors, inductors and capacitors which represent losses, coil windings and physical insulations respectively.

Depending on configuration and usage, difference power transformer may have difference types of windings. This consequently will have different winding response upon difference incoming high frequency signals (Pedersen et al. 2005). The difference can be noticeably seen in the typical construction between plain disc windings and interleaved disc windings type, in which the arrangement looks similar except the connection between coils and coil pairs. The difference connection cause different value of interturn capacitance in which the interleaved windings have higher series capacitance compared to plain winding (Hoogendorp et al. 2009).

TRANSFORMER WINDING MODEL

The winding model was fabricated and designed by Alstom and designed to have plain disc winding type. The winding model was set and installed at Tony Davies High Voltage Laboratory facility (Mohamed, 2010). The winding is filled with mineral type of transformer oil with the specification of BS148:1998 class 1. The main characteristic is it will not go into discharge or breakdown under an applied voltage up to 30 kV rms.

Figure 1 shows an example of winding cross-sectional view surrounds a metal type transformer core. The top and bottom of the winding is lining with end plates to reduce any abrupt voltage winding distribution. As for measurement point every pair of discs equipped with terminal points designated from 1 to 8.

The disc winding has several disc sections with 7 disc pairs and a total of 14 discs stacked onto each other connected to external terminals for winding response measurements from outside solid enclosure. The winding is made from a copper conductors wrapped around with crepe paper insulation type. It was made to meet the specification standard requirements of IEC27260. The core is a laminated cylindrical soft iron core and is connected to ground. The transformer winding is sealed and confined in a closed enclosure so as to have a closed transformer modes conditions similar to that of a real power transformer.

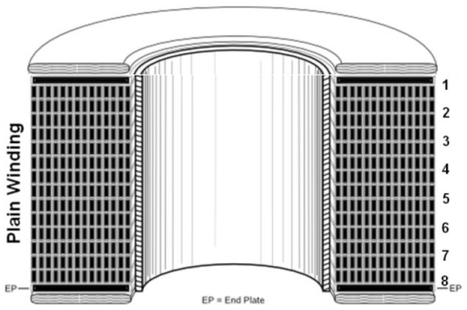

FIGURE 1. Winding crossectional view

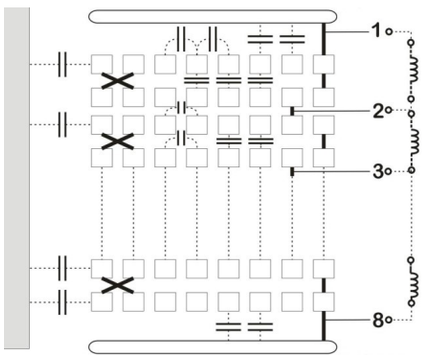

FIGURE 2. Disc winding connection

Figure 2 shows the connections between winding pairs and the equivalent arrangement of capacitance and inductance of the plain winding. This arrangement is based on the mechanical construction that represents the physical dimension and parameters of the transformer winding. In general, a transformer winding can be represented as a large inductor component in series with transmission lines hence winding resistance, while the paper dielectric material between the conductors can be represented as capacitances between adjacent conductors.

PLAIN WINDING SERIES AND SHUNT CAPACITANCE

Figure 3 shows an equivalent circuit arrangement of the capacitances of the plain disc winding. The equivalent capacitances are by considering inter-section capacitances K and inter-turn capacitances C_g. It is first assume that the disc coil has even distribution along the winding for the calculation of the capacitance. Therefore accumulated amount of energy within capacitive elements can be obtained by using sum of capacitances formula (Karsai et al. 1987).

Hence the resultant capacitance in one disc coil:

$$C_r = C_{gr} + K_r \tag{1}$$

Let n be the number of turns in each section, with N total number of sections per winding, thus the formula for inter-turn capacitance of the whole winding can be calculated using:

$$\sum_1^N C_{gr} = \frac{C_g}{Nn^2}(n-1) \tag{2}$$

In consequence, the resultant (K_r) inter-section capacitances can be calculated as follows:

$$\sum_1^N K_r = 4\frac{N-1}{N^2}K \tag{3}$$

As a result, the resultant series capacitance can be calculated from equations (2) and (3) described as:

$$C_r = \frac{1}{N}\left(\frac{n-1}{n^2}C_g + 4\frac{N-1}{N}K_r\right) \tag{4}$$

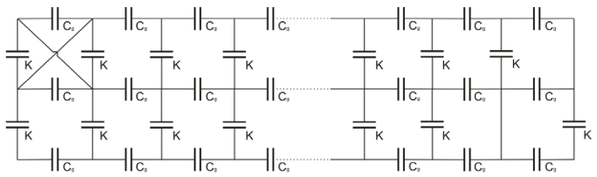

FIGURE 3. Equivalent series capacitance circuit for plain winding

Figure 4 shows the crossectional dimensions of a single phase plain disc winding.

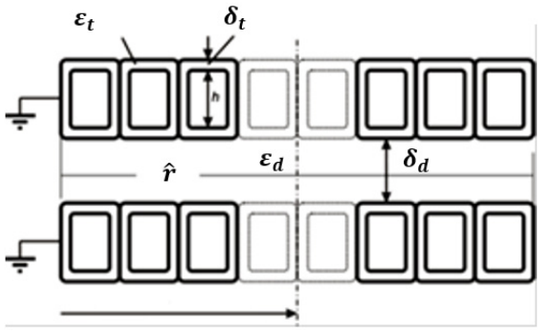

FIGURE 4. Winding dimensions

Where the followings are physical parameters; $\overline{D}$, mean winding diameter; h, copper conductor height; $\hat{r}$, radial diameter; δ_t inter-turn insulation thickness and δ_d distance between adjacent disc. The electrical parameters are of the followings;ε_d, permittivity of the oil; ε_t, resultant of inter-turn permittivity of the oil plus paper insulation.

Based on Figure 4, the inter-turn capacitance (C_g) and the resultant inter-section capacitance (K_r) can be determined using the following formulas (Karsai et al. 1987);

$$C_g = 27.8\overline{D}\,\frac{\varepsilon_t(h+2\delta_t)}{2\delta_t}\,10^{-12}\ F/turn \tag{5}$$

$$K_r = 27.8\overline{D}\,\frac{1}{3}\,\frac{\varepsilon_t\varepsilon_d(\hat{r}+\delta_d)}{2\delta_t\varepsilon_d+\delta_d\varepsilon_t}\,10^{-12}\ F/section \tag{6}$$

With reference to equations (1) to (6), the inter-turn capacitance and intersection capacitance are dependent parameters based on the arrangement of parallel conductors between disc sections.

REFLECTED AND TRANSMITTED WAVE IN TRANSFORMER WINDING

When a single travelling wave travels through a junction, some part of the wave will be reflected and some part of the wave will be refracted. The wave is measured either in voltage or current will change its magnitude based on the characteristics impedance of the line windings. Similarly for transformer windings, it consists of interconnected sections or junctions. Thus equation (7) and (8) show the reflected and transmitted wave model respectively (Mohamed 2010).

$$v' = V\frac{\mu}{v}\left[\frac{a+v}{a-\mu}e^{-at} - \frac{b+v}{b-\mu}e^{-bt} + \frac{(a-b)(v+\mu)}{(a-\mu)(b-\mu)}e^{-\mu t}\right] \tag{7}$$

$$v'' = V\left(1+\frac{\mu}{v}\right)\left[\frac{a}{a-\mu}e^{-at} - \frac{b}{b-\mu}e^{-bt} - \frac{(a+b)\mu}{(a-\mu)(b-\mu)}e^{-\mu t}\right] \tag{8}$$

Where a and b are arbitrary constant, μ and v are coefficients of the line impedance which effectively dependent on the value of effective inductance; L_o; of the winding with the following equations, with Z_1 and Z_2 as surge line characteristic impedance.

$$v = \frac{Z_1Z_2}{L_o(Z_2-Z_1)}\ ;\ \mu = \frac{Z_1Z_2}{L_o(Z_2+Z_1)}. \tag{9}$$

METHODOLOGY

INJECTION OF IMPULSE LIKE WAVESHAPE

Winding distributions is a voltage distribution along a winding in order to see the voltage developed in transformer windings. A non-invasive test can be conducted to performed the task with an injection of calibrated rectangular wave with infinitive wavetail. A rectangular waveshape of any mode can be represented as a:

$$V(t) = V(e^{-at} - e^{-bt}) \tag{10}$$

in which V represents time domain waveshape in either voltage or current mode, a and b are arbitrary constants. Equation (10) represents an impulse like waveshape which a and b will determine its wave characteristics. An example of the typical response represented by Equation (10) is shown in Figure 5.

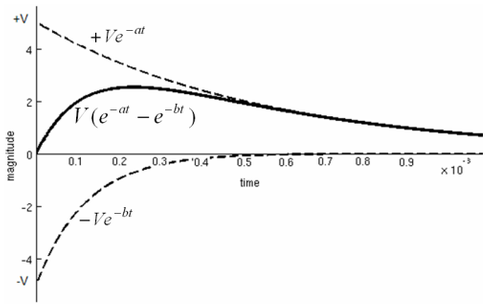

FIGURE 5. Impulse like travelling waves to represent rectangular waveshape, $a = 2\times10^3$ and $b = 9\times10^3$

Figure 5 represents an impulse like traveling wave based on the summation of waves represented by Equation (10). The wave can be determined by setting a suitable value of parameters *a* and *b*. The exponential wave of the top figure is by selecting the value of *b* to *1*, while the value of *a* can be selected to have various desired of its wavetail. While the bottom figure, by selecting the value of *a* to *1*, and selecting a suitale value of *b*, the waveshape can be expressed using equation $-Ve^{-bt}$.

Figure 6 shows the measurement setup for plain disc winding. The mentioned wave shapes were generated using typical programmable function generator from ArbStudio. The calibrated waves were injected at Terminal 1 (refer Figure 2) represents top of the winding and the resulting responses were measured at Terminal 2 to 8, to represent consecutive winding disc. The bottom of the windings was grounded to represent the attenuation signal at the end.

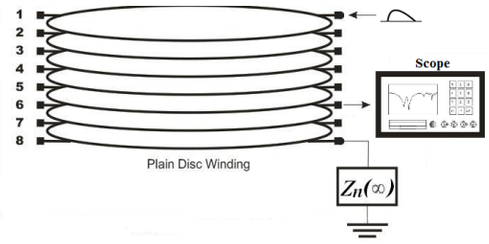

FIGURE 6. Experimental setup for plain disc winding

RESULTS AND DISCUSSION

INTER-SECTION AND INTER-TURN CAPACITANCES

Table 1 list out the detail parameters of the transformer plain winding model. By using these parameters, the interturn and intersection capacitances have been calculated using Equations (5) and (6).

Under normal circumstances, these values are very difficult to measure once the transformer has already sealed and enclosed. The only way to obtain its physical dimensions are from its manufacturer list of specifications and datasheets which could be troublesome sometimes.

The calculation of series capacitance and parallel capacitance were obtained based on two segments the interturn and intersection that results to total series capacitance and parallel capacitance respectively.

The determination of capacitances was based on the paper insulator gaps between winding conductors that wrapped around copper conductor in the transformer windings. The second gap was the existence of spacer between winding discs with a total of 7 gaps between 8 winding discs. These existence of gaps and paper insulators between winding conductors contribute to an equivalent capacitance.

The existence of winding core has contributed to capacitance to ground parameter that differs from difference level of transformer. However, the existence of this capacitance were considered to be as series capacitance between windings as formulated from Equation (5).

TABLE 1. Calculated inter-section and inter-turn capacitance for the winding model

No.	Parameters	Dimensions
1.	$\bar{D}$: winding diameter	87.5 mm
2.	h : height of copper conductor	7.0 mm
3.	$\hat{r}$: radial diameter of disc	85 mm
4.	δ_d: spacer between disc	3.0 mm
5.	ε_d: permittivity of oil	(2.5 – 7)
6.	δ_t: inter-turn insulation thickness	1.0 mm
7.	ε_t: inter-turn permittivity resultant	2.63
8.	N : Section total number	14
9.	n : Turn per-section number	14
10.	E_x: Intermidiary section under consideration	1 out of 14
11.	: No of oil ducts between windings	14
	Calculated Parallel and Series Capacitance (Plain Winding) C_g : K:	 28.79 pF 60.010 pF

INFINITE RECTANGULAR WAVE INJECTION

Figure 7 shows results based on the comparison between experimental data ($v''|_{measured}$) versus calculated equation model ($v''|_{calculated}$). A calibrated rectangular wave was set at Terminal 1 and the wave response was measured at the

same terminal. Both equation model and experimental results shows similarity to the time domain response. The results show a decay response on the wave tail based and high transition of its wavefront. This phenomenon was due to the travelling wave experiences damping factor due to the ground connection. Based on calculation the effective inductance of plain disc winding is very low; $L_o = 2.65$mH; which result in fast decay rate of its travelling wave. Base on the experimental result, it revealed that 45μs to decay to half value of the initial magnitude.

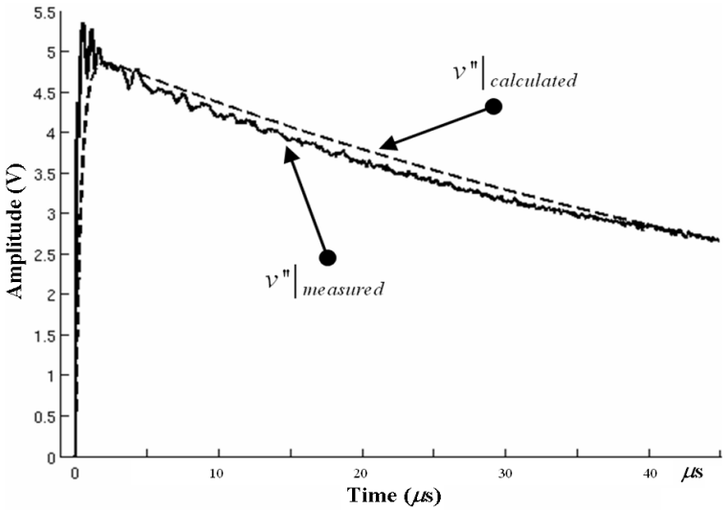

FIGURE 7. Comparison between calculated and measured for infinite rectangular wave response

The investigations were continued to the rest of the disc section along the disc winding. It was done by setting the same calibrated rectangular wave at different terminal positions along the transformer winding until the rest of the terminal points to the ground connection. The results were then compared with the model calculation to verify the overall winding distribution damping patterns only; this is due to the limitations of Equations (7) and (8).

Figure 8(a) and Figure 8(b) are the signals of the transmitted response at different measurement terminals for model calculation and real measurement respectively. It can be said that the high damping of the time domain response is highly affected by the injection point to the ground. Therefore, from analytical point of view, the approximation of effective inductance at various level can be estimated using the same solution and the results are shown in Table 2.

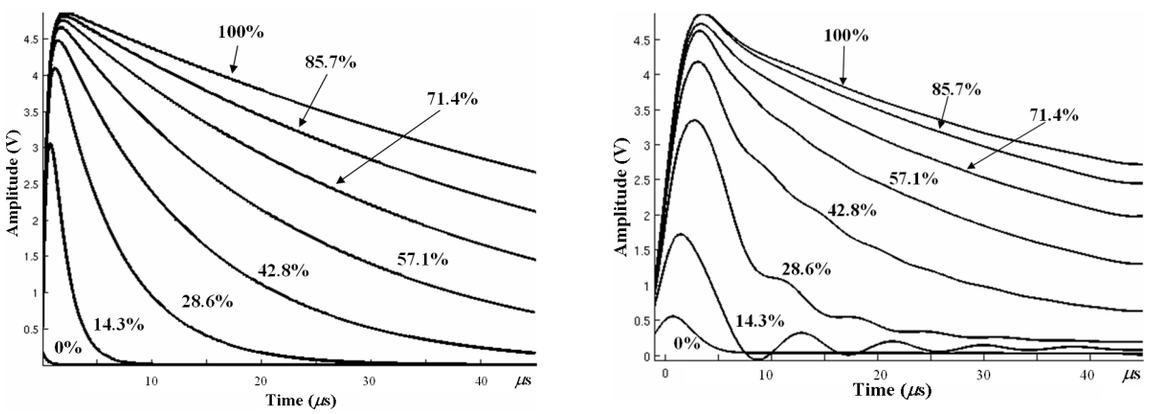

(a) Simulation

(b) Measurement

FIGURE 8. Response comparison between model calculation and measurement (0%: ground point; 100%: top winding).

TABLE 2. Table of effective inductance for Plain Disc Winding

Position from Neutral	Effective Inductance (*mH*)
100% (Bushing Point, Terminal 1)	2.65
85.7% (Terminal 2)	2.3
71.4% (Terminal 3)	1.7
57.1% (Terminal 4)	1.2
42.8% (Terminal 5)	0.8
28.6% (Terminal 6)	0.45
14.3% (Terminal 7)	0.15
0% (Terminal 8)	0.015

CONCLUSION

The research has presented a way to improved analytical formula from physical dimension with experimental data for certain physical parameters. Inductance and capacitance are the most prominent components exist in transformer windings, which may contribute to actual transformer winding response under transient condition. The typical technique in estimating the parameter such as interturn capacitance and intersection capacitance based on physical dimension still hold, which sometime proved difficult to be estimated accurately. However, in estimating the effective inductance with experimental data has proven to have a good approximation in comparison with transmitted and reflected wave equation model.

ACKNOWLEDGEMENT

The authors would like to thank Department of Electrical, Electronic and Systems Engineering, Advanced Power Engineering research group and Universiti Kebangsaan Malaysia for the support of the research activities.

DECLARATION OF COMPETING INTEREST

None

REFERENCES

Al-Kraimeen, Y. 2019. Parameter Determination and Modeling of Transformer Windings for Fast Transients Including Frequency Dependent Effects. Doctor of Philosophy, Department of Electrical and Computer Engineering, Western Michigan University.

Cheng, B. Wang, Z. & Crossley, P. 2020. Using Lumped Element Equivalent Network Model to Derive Analytical Equations for Interpretation of Transformer Frequency Responses. *IEEE Access*. 8: 179486–179496

D'Antonio, M. Chakraborty, S. & Khaligh, A. 2021. Planar Transformer With Asymmetric Integrated Leakage Inductance Using Horizontal Air Gap. *IEEE Transactions on Power Electronics*. 36(12):14014–14028.

Ding, Q. Yao, Y. Wang, B. Fu, J. Zhang, W. Zeng, C. Li, X. & Valtchev, S. 2020. A modified lumped parameter model of distribution transformer winding. *Global Energy Interconnection*. 3(2): 158–165.

Gustavsen, B. Martin, C. & Portillo, Á. 2020. Time-domain implementation of damping factor white-box transformer model for inclusion in EMT simulation programs. *IEEE Transactions on Power Delivery*. 35(2):464-472.

He, J. Tao, S. & Wu, H. 2020. A PEEC-based concise broadband physical circuit modeling method with parameter extraction for PCB inductive components. *IEEE Transactions on Power Electronics*. 35(10):10852–10862.

Hussain, M. K. & Gómez, P. 2023. Optimal dielectric design of medium voltage toroidal transformer with electrostatic shield under fast front excitation. *IEEE Transactions on Power Delivery*. 38(2):1395–1405.

Hoogendorp, G. Popov, M. & Sluis, L. V. D. 2009. Application of Hybrid Modeling for Calculating Interturn Voltages in Transformer Windings. *IEEE Transactions on Power Delivery.* 24(3):1742–1744.

Jafari, M. Malekjamshidi, Z. & Islam, M. R. 2021. Optimal design of a multiwinding high-frequency transformer using reluctance network modeling and particle swarm optimization techniques for the application of PV-linked grid-connected modular multilevel inverters. *IEEE Journal of Emerging and Selected Topics in Power Electronics*. 9(4):5083-5096.

Karsai, K. Kerenyi, D. & Kiss, L. 1987. Large Power Transformer. Elsevier Science Ltd.

Lewin, P. L. Golosnoy, I. O. & Mohamed, R. 2011. Locating Partial Discharge Sources in High Voltage Transformer Windings. *IEEE 2011 Electrical Insulation Conference, Annapolis, Maryland, United States*. 04–07 Jun 2011: 196–200 .

Luo, M. Dujic, D. & Allmeling, J. 2018. Leakage flux modeling of multiwinding transformers for system-level simulations. *IEEE Transactions on Power Electronics*. 33(3):2471–2483.

Mohamed, R. 2010. Partial Discharge Signal Propagation, Modelling and Estimation in High Voltage Transformer Windings, Doctor of Philosophy, School of Electrical and Computer Science, University of Southampton, SO17 1BJ .

Mohamed, R & Lewin, P.L. 2011. Lumped parameter model for high frequency partial discharge estimation in high voltage transformer. *10th WSEAS International Conference on System Science and Simulation in Engineering (ICOSSSE `11)*. Oct: 223–228.

Mukherjee, P. & Satish, L. 2018. Estimating the Equivalent Air-Cored Inductance of Transformer Winding From Measured FRA. *IEEE Transactions on Power Delivery.* 33(4):1620–1627.

Nia, M. S. S. Shamsi, P. & Ferdowsi, M. 2020. Investigation of Various Transformer Topologies for HF Isolation Applications. *IEEE Transactions on Plasma Science*. 48(2):512–521.

Pedersen, K. Lunow, M. E. Holboell, J. & Henriksen, M. 2005. Detailed high frequency models of various winding types in power transformers. *International Conference on Power Systems Transients (IPST05).* No. IPST05-100, June 2005